LAWRENCE
LIVERMORE
NATIONAL
LABORATORY

UCRL-JRNL-217247

Emerging Magnetism Arising from Self-Damage in (alpha) and (delta)-Pu

S. K. McCall, M. J. Fluss, B. W. Chung, G. F. Chapline, D. D. Jackson, M. W. McElfresh

November 22, 2005

Materials Research Society Symposium Proceedings

Emerging Magnetism Arising from Self Damage in α- and δ-Pu

S. McCall, M.J. Fluss, B.W. Chung, G.F. Chapline, D.D. Jackson, and M.W. McElfresh
Lawrence Livermore National Laboratory, Livermore, CA 94550 U.S.A.

ABSTRACT

As a consequence of the unusual nature of plutonium's electronic structure, point- and extended-defects are expected to, and do exhibit extraordinary properties[1]. Low temperature magnetic susceptibility measurements on Pu and fcc-Pu(Ga) show that the magnetic susceptibility increases as a function of time, yet upon annealing the specimen returns to its initial magnetic susceptibility. This excess magnetic susceptibility (EMS) arises from the α-decay and U recoil damage cascades which produce vacancy and interstitials as point and extended defects. The temperature of the first annealing stage defines a temperature (<35K) below which we are able to characterize the time and temperature evolution of the accumulating damage cascades as being a saturation function. The temperature dependence of the EMS is well described by a time independent, Curie-Weiss curve arising from a volumetric region surrounding each U damage cascade. This saturation picture also leads directly to a determination of the microscopic volume of the specimen that is affected by the frozen-in damage cascade. For our measurements in δ-Pu we calculate a diameter of the magnetically affected volume of ~250Å per damage cascade. This should be compared with an estimated volume that encloses the damage cascade itself (determined from molecular dynamics) of ~100 Å. Hence, the ratio of these volumes is ~8. The observed anomalous magnetic behavior is likely a consequence of the highly correlated nature of the electrons. Similarities with defects in hole-doped superconductors suggest a general phenomenon in strongly correlated electron systems, of which Pu may be a particularly unusual or special example.

INTRODUCTION

Plutonium occupies a unique position in the periodic table straddling the border between the itinerant electron light actinides and the more localized heavy actinides. It possesses a wealth of interesting properties including an anomalously low melting point, below which there are six distinct structural transitions at ambient pressure. Of particular note is the FCC δ-Pu phase, stable between 583K and 725K, which in addition to being the least dense phase has a negative thermal expansion. Alloying plutonium with several percent of a group IIIB metal (Al, Ga, In) kinematically stabilizes the delta phase to absolute zero. Owing to the technological importance of this phase, a variety of theoretical models have been developed to describe its properties[1-7]. Currently there is no complete model for plutonium, but at least one theory predicts a correct energy-volume diagram for all six phases[3]. However, a consequence of this theory, and several others[4, 8] is a prediction of a significant magnetic moment that is not observed experimentally[9]. Nonetheless, there is a broad agreement that understanding the spin and orbital moments of the 5*f* electrons is critical to explain the phase diagram of plutonium.

The 5*f* bands in plutonium are expected to be narrow, and consistent with this idea, recent measurements of the heat capacity show large electronic contributions to the specific heat[10] in

both α-Pu and stabilized δ-Pu. Similarly, all plutonium phases possess large magnetic susceptibilities suggesting they are on the border of becoming magnetic, and that slight perturbations may drive the system into a magnetic state.

From an experimental perspective, one of the challenges in working with plutonium is its radioactivity. Plutonium decays via emission of a 5.04 MeV α-particle and corresponding 85.8 keV U recoil. During this event, the alpha particle travels about 10 μm, transferring most of its kinetic energy to the electrons, through electron-hole pair formation, although near the end of its path (~0.8 μm) it undergoes atomistic collisions with the Pu lattice and creates approximately 250 sparsely distributed vacancies and interstitials, or Frenkel pairs. By contrast, the recoiling U tumbles through the lattice colliding with other atoms and initiating much denser cascades of Frenkel pairs. Though this recoil travels only about 12 nm, it generates approximately 2300 such pairs of vacancies and interstitials[11]. Most of the defects recombine during the next several tens of picoseconds as the lattice rapidly cools, leaving only 10-30% of the initial vacancies and interstitials spread throughout the volume. We report observation of increasing magnetic susceptibility due to this self-damage in α-Pu and δ-Pu. Previous work[12-14] has examined the impact of self damage on resistivity and volume in plutonium specimens. In each case, the resistivity systematically increased as a function of damage. More recently, the temperature dependence of the specific resistivity of vacancies and vacancy clusters in Ga stabilized δ-Pu was shown to exhibit a -ln(T) temperature dependance, which may imply a defect-induced Kondo-like behavior[15], analogous to that seen in hole doped superconductors subjected to electron irradiation[16]. Here we report the discovery and characterization of time and temperature dependent magnetic susceptibility caused by accumulating damage in α-Pu and δ-Pu (4.3 at.%Ga) which is fully reversible through thermal annealing.

This provides a unique opportunity to investigate the effects of continuously doping a specimen simply by observing the behavior as a function of time. Furthermore, dilute doping levels difficult to achieve by chemical doping can be investigated systematically and reversibly by annealing out the damage.

EXPERIMENT

A batch of Pu (99.98% pure), melted and electro-refined within the last two years, was used to manufacture two specimens: α-Pu and δ-Pu stabilized with 4.3 atomic percent Ga. The samples were mechanically shaped to 1x2x2 mm bars, and then mechanically and chemically cleaned of oxide, yielding specimens of 56.8 mg and 45.4 mg respectively. The isotopics were determined by inductively coupled plasma mass spectroscopy, where the primary constituent is ^{239}Pu (93.7%), with smaller concentrations of ^{240}Pu (5.86%) and ^{238}Pu (0.17%) contributing appreciably to the radioactivity of the sample. The balance of the specimens included the following magnetic impurities in atomic ppm: Fe(231), Ni(24), Cr(12) and Mn(10). To contain radioactive spall, the specimens were coated with ~5 microns of polyimide and cured at 350K for several hours, well below the 390K α to β Pu phase transformation.

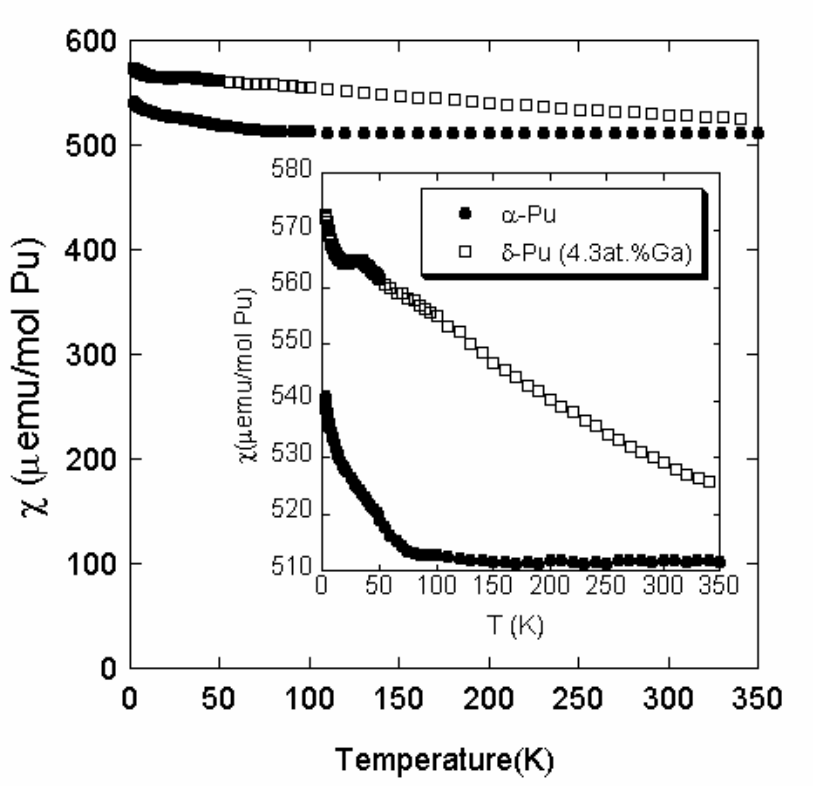

Figure 1. Magnetic susceptibility for thermally annealed specimens emphasizing the temperature independent Pauli contributions. The inset shows details of the temperature dependent contributions, which are dominated by low levels of impurities (see text for details).

Each encapsulated specimen was then mounted in a well-characterized cartridge-brass tube (20cm long), hermetically sealed under an atmosphere of helium at ambient temperature, and measured using a commercial SQUID magnetometer (Quantum Design MPMS-5) where the small background contribution of the tube could be readily subtracted from the raw data. The total background contribution varied only weakly as a function of temperature and magnetic field, and never exceeded one percent of the overall signal. Furthermore, many of the results presented here are essentially differential measurements—changes in magnetic susceptibility as a function of time—so the background contribution effectively cancels itself. In addition to contributing a minimal background signal, the large thermal conductivity of the brass permits the tube to act as a heat sink for the sample at low temperatures, helping to ensure thermal stability. The temperature of a duplicate sample holder with the sample replaced by a heater and thermometer showed the maximum self-heating effect was roughly 50 mK at 2K. At each new temperature, care was taken to ensure that the specimen and tube were in thermal equilibrium before measurements began, and then repetitive measurements showed no systematic trend in the magnetic susceptibility indicative of a thermal lag between the system thermometer and the sample.

The magnetic susceptibility, defined as $\chi(T)=M/H$, of freshly annealed (350K for 1 hour) α-Pu and δ-Pu specimens was measured for $2K<T<350K$. The dominant contribution to $\chi(T)$ in both specimens is the temperature independent Pauli susceptibility, and this is emphasized in Fig. 1 where both plots are relatively flat when shown at full scale. The inset of Fig. 1 expands the ordinate axis to reveal the details of the temperature dependent contributions for each

specimen. Even on this enhanced scale, the temperature independence of the magnetic susceptibility for α̃-Pu is clear above approximately 100K where it remains essentially constant at 511±1 μemu/mol, comparable to values published elsewhere[17-19]. The lower temperature region reveals a small temperature dependant contribution of only about five percent of the overall signal. Below 40K, this contribution fits well to a modified Curie-Weiss law with an effective magnetic moment of $4.16\mu_B$/Fe, somewhat less than the $5.92\mu_B$/Fe ($4.90\mu_B$/Fe) expected were all the Fe impurities effectively trivalent(divalent) with S=5/2 (3/2), but not unreasonable when compared to Fe dissolved in other host metals[20]. An additional, smaller feature occurs near 60K, which might be attributed to a very small contribution of a second intermetallic phase such as Pu_6Fe.

The magnetic susceptibility for δ-Pu is more complex, though still dominated by a temperature independent Pauli term, as observable in Fig. 1. The inset of Fig. 1 shows that the overall magnitude changes less than 10% between 350K and 2K, yet there are several noteworthy features. There is a low temperature Curie tail consistent with that observed in the α̃-Pu sample. In addition to this, there is a small peak at ~33K, with a weak temperature dependant contribution at higher temperatures. This contribution could be described by a second phase of $PuGa_{3-x}$ ($0 \leq x \leq 1$) at the level of a fraction of a percent. Recent studies of $PuGa_2$ and hexagonal $PuGa_3$ show that they order antiferromagnetically at 74K and 24K respectively, with the hexagonal $PuGa_3$ phase stabilized by annealing at 800°C[21, 22]. Incomplete annealing of the delta-stabilized phase could easily result in a contribution of this magnitude. Furthermore, the weak temperature dependence at temperatures above ~50K is quite similar to previous observations of Ga stabilized δ-Pu[23] which did not extend to sufficiently low temperatures to rule out second phases. Finally, additional support for the dominance of the Pauli susceptibility is the low temperature magnetization, which in each case is very linear.

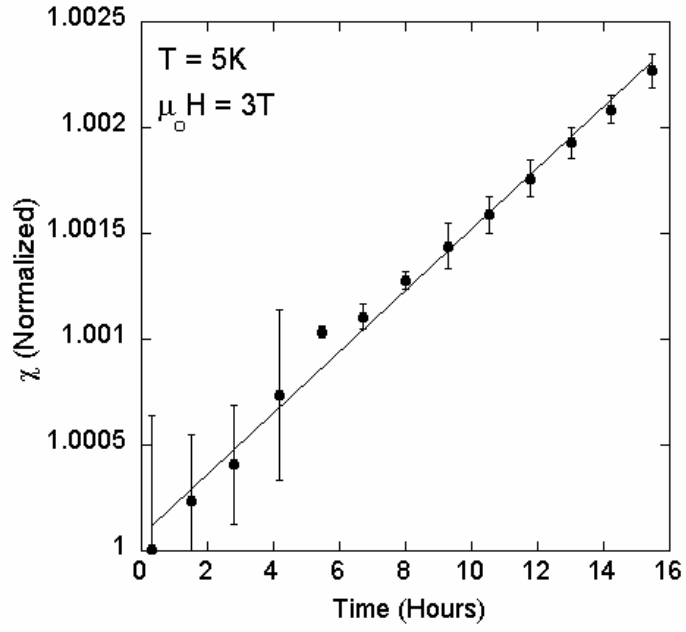

Figure 2. The initial increase in the isothermal magnetic susceptibility as a function of time for α-Pu.

At low temperatures, the isothermal magnetic susceptibility increases as a function of time as shown in Fig. 2 for freshly annealed α-Pu at 5K. Here the initial slope is a few hundred parts per million over the course of a day, while the initial rate observed in the δ-Pu specimen is several times larger. In each specimen, brief anneals at 350K returned the magnetic susceptibility to the initial state, suggesting that the excess magnetic susceptibility (EMS) arises from the radiation induced defects, and not the accumulation of decay products—principally uranium and helium. To confirm this result, damage-accumulation isochronal-annealing studies were performed which are explained in detail elsewhere[15, 24]. The results of these studies show that for temperatures less than 35K, the specimens are below Stage 1 annealing, meaning that the defects and vacancies are effectively frozen in place. Upon heating above 35K, near vacancy-interstitial pairs begin to annihilate, and as the temperature continues to increase, a complex series of additional annealing stages involving the thermal activation of interstitials, vacancies, and more extended defect aggregates transpires. Finally, at about 315K and 300K for α-Pu and δ-Pu respectively, Stage V is achieved, corresponding to complete annealing of the remaining defects. At this point, the decay products (primarily U and He) remain, but their contribution to the overall magnetic susceptibility is vanishingly small, and the specimen returns to the "undamaged" state. Indeed, measurements at 5K made several months apart on the same specimen immediately after annealing at 350K gave the same values of the magnetic susceptibility within experimental uncertainty. By observing the damage accumulation at low temperatures, coupled with the ability to wash away the damage with anneals above room temperature, a systematic study of how the EMS evolves with damage may be undertaken.

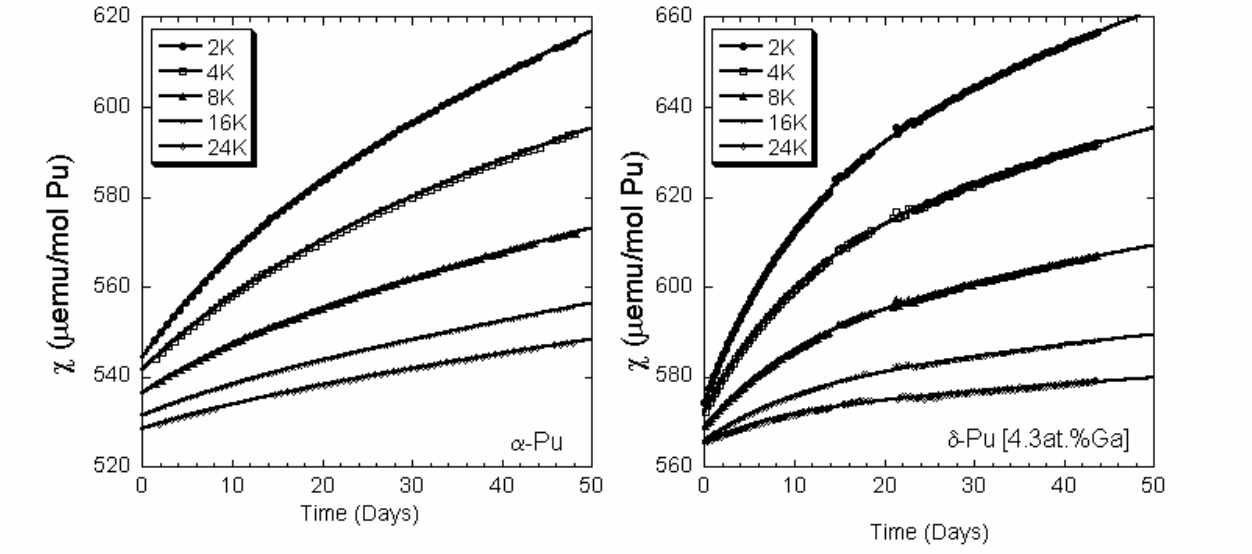

Figure 3. Representative isotherms illustrating the time (damage) dependant magnetic susceptibility for α-Pu (left) and δ-Pu (right). The points represent raw data while the lines are best fits to eq. (2) in the text.

RESULTS

For the two specimens, the magnetic susceptibility was measured as the temperature was repeatedly cycled between 2K and 30K for a period exceeding 40 days. Over time, the initial linear time dependence of the magnetic susceptibility decreases, and a more complex behavior evolves. At first, a simple exponential term was used to fit the EMS for the case of α-Pu leading to the following equation:

$$\chi(t,T) = \chi_i(T) + \chi_{EMS}(T)\left(1 - \exp\left[-t/\tau(T)\right]\right) \qquad (1)$$

where τ is some characteristic time. This equation fits can be fit to all 32 isotherms provided that τ is permitted to vary, and results in a τ(T) that increases linearly with temperature from 30 Days at 2K to 55 Days at 20K, above which it remains essentially constant. However, equation (1) does not fit well the δ-Pu(3.4at.%Ga) isotherms, implying that a more complex model is required. An additional term, linear in time was added, thus changing the equation to:

$$\chi(t,T) = \chi_i(T) + \chi_{XS}(T)\left[1 - \exp(-t/\tau)\right] + \chi'_D(T)t \qquad (2)$$

where the EMS is now separated into two terms: $\chi_{XS}(T)$ represents the coefficient of a term that saturates at sufficiently long times, while the prime on the third term, $\chi'_D(T)$, emphasizes that the units of that coefficient are per unit time. This equation fits all 37 isotherms for the δ-Pu

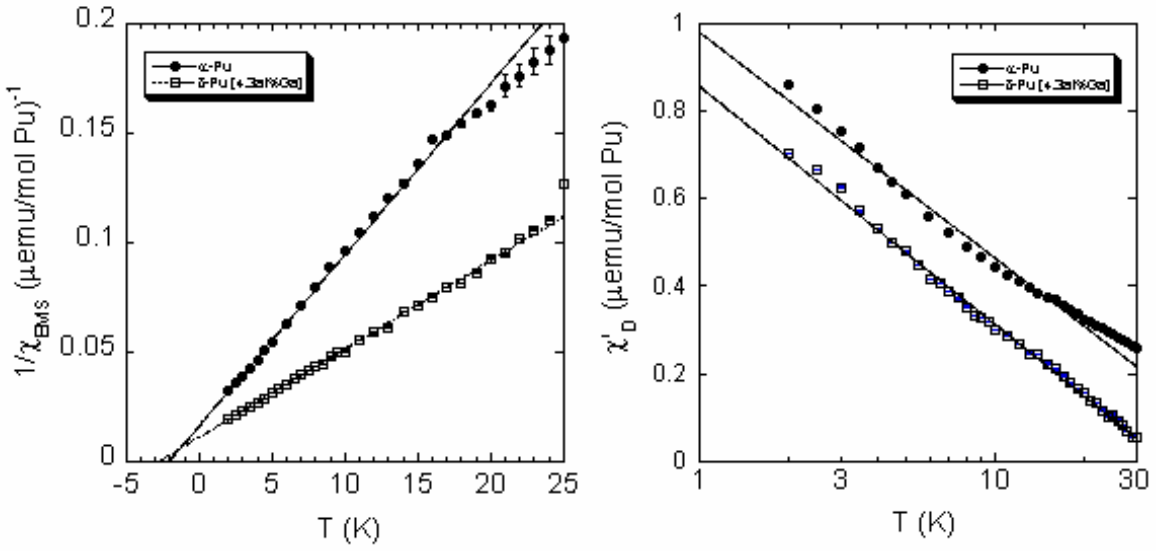

Figure 4 The temperature dependent contributions for α-Pu and stabilized δ-Pu. (a) The inverse magnetic susceptibility for both specimens showing a good fit to a Curie Weiss law. (b) The second time dependent contribution obeys a –ln(T) temperature dependence

specimen with a single characteristic time: τ=11.6 ± 0.3 days. Returning to the case of α-Pu, the 32 isotherms also fit with a constant τ=15.8 ± 0.5 days, removing the temperature dependence of τ, while not increasing the degrees of freedom required to fit the $\chi(t,T)$ data. Several representative plots of the data for the two allotropes are shown in Fig. 3, where the data are represented as points, and best fits to equation 2 are plotted as lines.The two distinct time contributions suggest that the damage-spawned contributions to the magnetic susceptibility arise from at least two distinguishable types of effects. This is further clarified by an examination of the temperature dependence for each contribution. The temperature dependence of $\chi_{XS}(T)$ is plotted in Fig. 4(a) as $1/\chi_{XS}(T)$ vs. T, illustrating that it obeys a Curie-Weiss law: $\chi = C/(T-\theta)$ and that both allotropes have similar paramagnetic Weiss temperatures, shown by the x-intercept: $\theta \sim -2K$. The negative value of the Weiss temperature indicates antiferromagnetic fluctuations, with the magnitude providing a characteristic energy scale. The best fit of the slope for each line in Fig. 4(a) permits extraction of Curie constants, which correspond to 127.9 μemu/mol·K for α-Pu and 248.1 μemu/mol·K for δ-Pu. From the decay rates of the Pu, and the time constants obtained above, in the dilute limit ($t<<\tau$), each α-decay generates an effective moment of 22.5μ_B in α-Pu and 36.8μ_B per α-decay in δ-Pu. As an added note, the fits of Fig. 4(a) require no temperature independent term (*i.e.* the χ_o term in a modified Curie-Weiss fit). This is significant because it suggests that the band structure of plutonium is not appreciably altered by the damage cascades, or by the evolving local moments. Fig. 4(b) shows the contribution of the $\chi'_D(T)$ term for both allotropes, where the temperature is plotted on a log scale to illustrate the $-\ln(T)$ behavior. The slopes of each phase are strikingly similar, suggesting a common interaction independent of the details of the crystal structure.

While there are striking similarities in the overall behavior of the radiation damage in each allotrope, the relative magnitudes of the different effects may lend some additional insight into the underlying properties. With this in mind, Fig. 5 shows representative plots of the magnetic susceptibility as a function of time, with each decomposed into the respective components. The data sets were obtained at 4K, and the ordinate axes span the same range so that direct comparisons of magnitudes between the two plots may be considered. In both cases, the time dependence of the $\chi_{xs}(T)$ term is the dominate contribution at short times when the damage is relatively dilute, whereas the $\chi'_D(T)\cdot t$ contribution dominates at long times. If one assumes that a region influenced by damage is not further altered by additional damage, this suggests that $\chi_{XS}(T)$ may reflect an extended effect that saturates after modest times. By contrast, the $\chi'_D(T)$ contribution shows no sign of saturating over the measurement time, suggesting a much more localized effect. In comparing these two contributions, probably the most obvious observation is the significantly shorter time required for $\chi'_D(T)\cdot t$ to surpass $\chi_{xs}(T)$ in the case α-Pu (~25 Days) as compared to stabilized δ-Pu (~75 Days). If $\chi'_D(T)$ indeed arises from a short range effect immediately surrounding a vacancy or interstitial, then perhaps the Ga atoms which stabilize the delta phase also act as effective defects, and mask the influence of new damage generated defects, thus having a lesser overall impact on the magnetic susceptibility.
As further evidence for evolving local moments, measurement of the differential magnetization due to self-damage is presented in Fig. 6 for stabilized δ-Pu. The inset shows the isothermal magnetization (T=2K) for both the damaged (~50 days below Stage I annealing) and annealed specimen. In both cases, the dominant term remains the Pauli susceptibility, which is expected to remain linear with the applied magnetic field for experimentally obtainable magnetic fields. However, the overall increase in magnetization exceeds ten percent of the initial value. The

difference between these two values, ΔM = M(Aged) – M(Annealed), is the excess magnetization that arises from the self-damage. Clearly, there is an appreciable deviation from linear behavior in ΔM, and the line represents a single parameter fit to a Brillouin function assuming J=5/2 and g=2/7, which are the values observed for Sm^{+3}, the 4*f* analog of Pu^{+3}. With these assumptions, the fit equates to 1 out of 1750 atoms contributing a full moment, or an average of about 100 local moments per α decay. These assumptions are very likely insufficient to properly describe the effect of defects as trivalent Sm is well described by Russell-Saunders coupling (LS), whereas the strong spin-orbit interaction among the 5*f* electrons indicate that a jj coupling or at least intermediate coupling scheme is probably a better description for Pu. Furthermore, the extended radii of the 5*f* orbitals as compared to the 4*f*s lead to the expectation of much more significant crystal field effects. Finally, the two component fit used for the magnetic susceptibility is not addressed at all in this picture. So, while the details may not be clear, the magnetic field dependence of the damage-induced magnetization is far more consistent with localized behavior (Brillouin like) than the linear behavior of a simple Pauli system, as in for the annealed specimen.

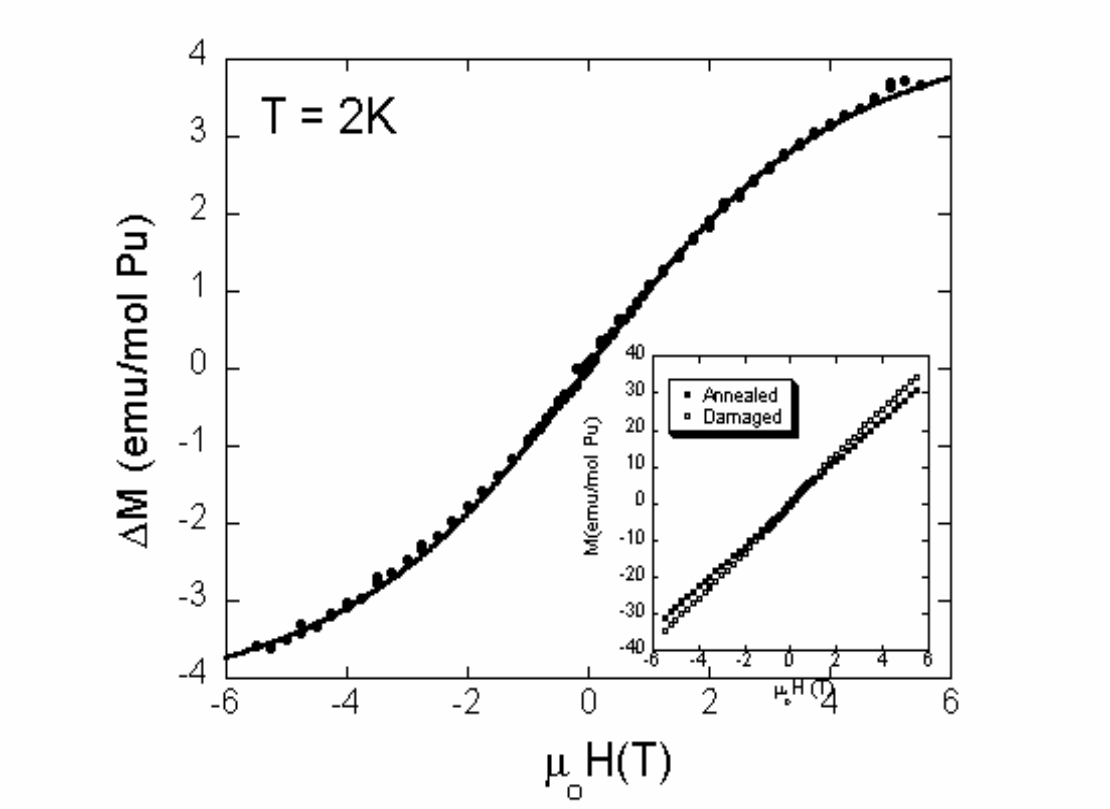

Figure 5. The differential magnetization: M(Damaged) – M(Annealed) representing the damage induced contribution for δ-Pu(4.3at.%Ga). The curve is a single parameter fit to a Brillouin function assuming J = 5/2 and g=2/7.

CONCLUSIONS

An excess magnetic susceptibility evolving with time has been observed at low temperatures in both α-Pu and stabilized δ-Pu [4.3at.%Ga]. Isochronal annealing studies show that this EMS may be removed by annealing at temperatures near 350K, demonstrating that the EMS arises from defects produced by radiation damage, and not the resulting decay products, which are not changed by annealing. The time evolution of the EMS may be decomposed into a two-component model, where each time component has a distinct temperature dependence. The explicit temperature dependence of these terms argues in favor of developing localized moments. The dominant term at short times, $\chi_{XS}(T)$, fits well to a Curie Weiss law, where in the dilute limit each α-decay creates an additional effective magnetic moment of $22.5\mu_B$ and $36.8\mu_B$ for α-Pu and δ-Pu respectively. Both allotropes also have a small negative paramagnetic Weiss temperature, suggesting the presence of antiferromagnetic fluctuations with an energy scale on the order of 2K. At longer times, a term linear in time begins to dominate the EMS, and it has a –ln(T) temperature dependence, with a common slope for both allotropes. This behavior is reminiscent of the resistivity contribution due to individual vacancies observed in δ-Pu, which also has a –ln(T) temperature dependence and was suggested as an indicator of defect induced Kondo behavior[15]. Finally, low temperature differential magnetization measurements reveal that the damage induced magnetization fit well to a Brillouin function. This is strong evidence that radiation damage is producing localized moments in plutonium where there were none in the undamaged state. Work remains to be done in understanding where these moments are arising, just how localized they are, and what influence they have on the overall electronic properties of plutonium.

ACKNOWLEDGEMENTS

This work was performed under the auspices of the U.S. Department of Energy by University of California, Lawrence Livermore National Laboratory under Contract W-7405-Eng-48.

REFERENCES

[1] A. O. Shorikov, A. V. Lukoyanov, M. A. Korotin, V. I. Anisimov, *Phys. Rev. B* **72** 024458 (2005).
[2] P. Soderlind, A. Landa, B. Sadigh, *Phys. Rev. B* **66** 205109 (2002).
[3] P. Soderlind, B. Sadigh, *Phys. Rev. Lett.* **92** 185702 (2004).
[4] S. Y. Savrasov, G. Kotliar, *Phys. Rev. Lett.* **84** 3670 (2000).
[5] S. Y. Savrasov, G. Kotliar, E. Abrahams, *Nature* **410** 793 (2001).
[6] J. Bouchet, B. Siberchicot, F. Jollet, A. Pasturel, *J. Phys.: Condens. Matter* **12** 1723 (2000).
[7] A. B. Shick, V. Drchal, L. Havela, *Europhys. Lett.* **69** 588 (2005).
[8] G. Robert, A. Pasturel, B. Siberchicot, *J. Phys.: Condens. Matter* 8377 (2003).
[9] J. C. Lashley, A. Lawson, R. J. McQueeney, G. H. Lander, *Phys. Rev. B* **72** 054416 (2005).
[10] J. C. Lashley, A. Migliori, J. Singleton, R. McQueeney, M. S. Blau, R. A. Pereyra, J. L. Smith, *JOM-Journal of the Minerals Metals & Materials Society* **55** 34 (2003).
[11] W. G. Wolfer, *Los Alamos Science* **26** 274 (2000).
[12] D. A. Wigley, *Proc. R. Soc. London, A* **284** 344 (1965).
[13] J. A. Lee, K. Mendelssohn, D. A. Wigley, *Phys. Lett. A* **1** 325 (1962).

[14] M. J. Mortimer, J. A. C. Marples, J. A. Lee, *Int. Met. Rev.* **20** 109 (1975).
[15] M. J. Fluss, B. D. Wirth, M. Wall, T. E. Felter, M. J. Caturla, A. Kubota, T. D. de la Rubia, *J. Alloys Compd.* **368** 62 (2004).
[16] F. Rullier-Albenque, H. Alloul, R. Tourbot, *Phys. Rev. Lett.* **91** 047001 (2003).
[17] J.-M. Fournier, R. Troc, Bulk Properties of the Actinides, in: A. J. Freeman, G. H. Lander (Eds.), Handbook on the Physics and Chemistry of the Actinides, vol 2, North-Holland, New York, 1985.
[18] A. Blaise, J.-M. Fournier, *Solid State Commun.* **10** 141 (1972).
[19] C. E. Olsen, A. L. Comstock, T. A. Sandenaw, *J. Nucl. Mater.* **195** 312 (1992).
[20] A. M. Clogston, B. T. Matthias, M. Peter, H. J. Williams, E. Corenzwit, R. C. Sherwood, *Physical Review* **125** 541 (1962).
[21] P. Boulet, E. Colineau, P. Javorsky, F. Wastin, J. Rebizant, *J. Alloys Compd.* **394** 93 (2005).
[22] P. Boulet, E. Colineau, F. Wastin, P. Javorsky, J. C. Griveau, J. Rebizant, G. R. Stewart, E. D. Bauer, *Phys. Rev. B* **72** 64438 (2005).
[23] S. Meot-Reymond, J. M. Fournier, *J. Alloys Compd.* **232** 119 (1996).
[24] S. McCall, M. J. Fluss, B. W. Chung, M. W. McElfresh, G. F. Chapline, D. J. Jackson, *Materials Science Transactions* **8** 35 (2005).